A novel polyaniline titanium oxide sawdust composite adsorbent for polychlorinated biphenyls

Fredrick Okumu, Mangaka Matoetoe[*]**, Olalekan Fatoki**

Department of Chemistry, Cape Peninsula University of technology, P.O. Box 652, Cape Town 8000, South Africa

Email address:

lellangm@gmail.com(M. Matoetoe)

Abstract: Polyaniline /sawdust /titanium oxide (PANI/SD/TiO$_2$) composite was chemically synthesised by insitu polymerization of aniline monomer in acidic medium containing sawdust and titanium oxide. The structure and morphological variations of PANI/SD/TiO$_2$ composite were interrogated by means of spectroscopy (FTIR, UV-visible, thermal gravimetric (TG) analyzer, X-ray diffraction (XRD), scanning electron microscope (SEM) and transmission electron microscope (TEM). Noticeable spectral and morphological changes were observed compared to pristine PANI thus, strongly suggesting chemical interaction between compounds present in the composite. Batch experiments were adopted in examining the adsorption kinetics and isotherm of selected polychlorinated biphenyl (PCB) congeners (PCB: 28, 52 and 101). Results indicate that PANI/SD/TiO$_2$ can be used as a novel, effective and low-cost adsorbent material for lower Chlorinated PCB remediation (PCB 28). Adsorption equilibrium studies followed Freundlich for PCB 52 and Langmuir models for PCB 28 and 101. While the adsorption kinetics were best described by pseudo-second-order (PCB 28 and PCB 52) and intraparticle diffusion models (PCB 101).

Keywords: Polychlorinated biphenyl, Polyaniline, Sawdust, Adsorption, Kinetics

1. Introduction

Polychlorinated biphenyls (PCB's) are known harmful chemicals whose presence in water is undesirable due to their toxicity to human beings. Therefore, environmental security is one of the fundamental requirements of our well-being. Nowadays, they are various ways which are utilized to minimize the amount of PCB's in the environment. However, the stability of these compounds in the environment necessitates remediation actions. Notable Remediation methods involves adsorption, chemical decomposition and electrochemical degradation, the former being the most popular due to cost efficiency. Activated carbon is a popular adsorbent for removal of polar pollutants from wastewater [1] such as PCBs. However, the activated carbon has high regeneration cost, poor mechanical rigidity and is expensive compared to usage of agricultural wastes [1] and this has limited its wider applications. To overcome these problems, they have been an increased usage of low cost adsorbents such as fly ash in remediation [2].

For several years heterogeneous-conducting polymer composites have drawn a lot of environmentalist attention as alternative adsorbents [3, 4]. This has been due to their wide variation in functionality, surface area, porosity and the ease of regeneration which has resulted in the usage of polymeric resins for removal of specific pollutants from wastewater [5, 6, 7]. Various polymeric adsorbents have been investigated and different adsorption mechanisms have been proposed [8, 9, 10]. The use of these polymeric adsorbents for the treatment of effluents containing benzenoid compounds has been widely studied [11].

Polyaniline (PANI) is one of these polymers that have attracted considerable attention, due to its unique, easily controlled, reversible properties by both charge-transfer doping and protonation. These electrical, electrochemical and optical properties coupled with good stability make PANI potentially attractive for application in various fields. Besides the many other interesting properties, PANI exhibits relatively high surface area and porosity [12,13] and has been reported as an adsorbent for adsorption of proteins[14,15], Dyes [16,17], cations [18] and DNA [19–21]. The use of pristine PANI powder as adsorbent, however, could be limited by the polymer surface area and complicated by diffusion processes. This drawback necessitated further functionalization of PANI resulting in extensive research in the preparation of PANI composites

with inorganic, organic particles and agricultural biomass. For example, polyaniline coated sawdust (PANI/SD) hybrid has been effectively used in removal of metals [22, 23], anions [24], and dyes [25, 26] from wastewaters. They are also reports of adsorption of trace naphthalene compounds from drinking water preparation [27, 28].

The major drawback of adsorption techniques in remediation is accumulation and disposal of the spend adsorbents. This study involved a synthesis of a composite that consists of a polymer (PANI), biomass (Sawdust) and catalyst (titanium oxide). Presence of the catalysts is to enable regeneration of the composite thus overcoming solid waste disposal. The spectrophotometric interrogation of composite (PANI/SD/TiO$_2$) is done to gain an insight into the interaction of the components. This composite can be recycled as an additive in paint manufacturing [29]. The application of the composite as an adsorbent is tested on selected polychlorinated biphenyl congeners of interest (PCB 28, PCB 52, and PCB 101). Possible kinetic mechanisms and adsorption models of the congers were investigated.

2. Experimental

2.1. Material and Reagents

Aniline (99 % purity, Sigma Aldrich) was doubly-distilled before use under reduced pressure and stored at a low temperature (-4^{0}c), Hydrochloric acid (37 %), Analytical grade ammonium persulfate ((NH$_4$)$_2$S$_2$O$_8$, (APS)), sawdust particles in the form of fine particles were used directly without additional treatment. N, N-dimethylformamide, (DMF) (anhydrous, 99.8 %, analytical grade), Titanium dioxide (TiO$_2$) from Fluka Analytical. Acetonitrile (HPLC grade), phosphate buffer (PBS), pH 7.4, Analytical grade argon (Afrox, South Africa) was used to degas the system. Tetrabutylammonium perchlorate, (TBAP; Sigma Aldrich, electrochemical grade) was also used without further purification. Deionized water was used for aqueous solution preparations. PCBs (PCB 28, PCB 52 and PCB 101) were purchased from Dr. Ehrenstorfer (Augsburg, Germany). All PCB stocks were prepared freshly in 0.1 M TBAP/ACN/PBS 80:20 v/v before use.

2.2. Square Wave Quantification of Polychlorinated biphenyls

Square wave Voltammetry was used to quantify PCBs using a Bas 100W electrochemical analyser from Bioanalytical systems Inc (West Lafayette, IN). Experiments were run using a three electrode system that consists of a glassy carbon electrode (GCE) as the working electrode (A = 0.071 cm^2) and 3 mm of diameter, a platinum wire from Sigma Aldrich and Ag/AgCl (3 M NaCl) electrodes from BAS were used as auxiliary and reference electrodes, respectively. Alumina micropowder and polishing pads were obtained from Buehler, IL, USA and were used to polish the GCE. All potentials were quoted

with respect to Ag/AgCl. All experimental solutions were purged with high purity argon gas and blanketed with argon atmosphere during measurements. The experiments were carried out at room temperature (25 °C).

2.3. Preparation of PANI/SD/TiO$_2$

Titanium dioxide (TiO$_2$) functionalized polyaniline coated sawdust (PANI/SD/TiO$_2$) was synthesized as follows; In 5.0 g of sawdust (SD) that has been soaked in 45 mL of 1 M HCl, for 10 minutes, aniline was added to make a final concentration of 0.02 M followed by addition of 10 mL 1M of TiO$_2$ and the mixture was stirred for few minutes (about 2 minutes). Finally 2.5 g of APS was added to the mixture with continuous stirring for 24 h at room temperature while polymerization occurred. The composite formed was collected by filtration on a Buchner funnel using a water aspirator and washed thoroughly with deionized water to remove traces of monomers and HCl then left to dry at room temperature.

2.4. Spectrophotometric Characterization of the Composite

The DMSO solutions of the composites, UV-visible spectra were done on a Nicolet evolution 100 spectrophotometer in the range of 200-800 nm using a 1-cm path length quartz cuvette while the Infrared spectra were recorded on a Perkin Elmer model Spectrum 100 series spectrometer in the range of 400-4000 cm^{-1}. The SEM micrographs of samples mounted on aluminium studs using conductive glue and drop coated with thin layer of carbon before analysis were obtained on a JEOL JSM-7500F scanning electron microscope. TEM images of samples which were suspended in dilute ethanol onto a carbon-coated copper grid and allowed to air dry were performed on a HR-TEM (Tecnai, G2 F20 X-Twin MAT) transmission electron microscope at an accelerating voltage of 200 kV. X-ray diffraction patterns were collected on a Bruker-Axs D8 advance XRD with Cu Kα radiation operating at 40 kV and 40 mA. The XRD spectra were recorded in the range of 10 ° to 90 °C. TGA analysis were run on a thermogravimetric (TG) analyzer (Model: Pyris 6, Perkin Elmer) at the heating rate of 10 °C/min in a nitrogen atmosphere from 30 ° to 400 °C.

2.5. Adsorption Experiments

For each experimental run, 10 mL of PCB of known concentration and 0.05 g of the synthesized PANI/SD/TiO$_2$ were taken in a 50 ml glass beaker. The mixture was left unstirred at room temperature. 0.5 mL of the samples was withdrawn at 15 minutes time intervals for 1.75 h and supernatant liquid portions centrifuged for 10 min. The supernatant was then brought into an electrochemical cell and the equilibrium concentrations of the PCBs (PCB 28, PCB 52 and PCB 101) determined by square wave voltammetry (SWV) technique, using an electrochemical analyzer (BAS 100W). The adsorbed amounts of PCB were

calculated using the equation 1 below:

$$q_t = \left(\frac{C_o - C_e}{m} \right) v \qquad (1)$$

Where C_o and C_e are the initial and equilibrium concentrations of PCB (molL^{-1}), m is the mass of PANI/SD/TiO$_2$ (g), q_t is the amount adsorbed (mol g^{-1}) and V is the volume of solution (L).

3. Results and Discussion

3.1. Compounds Appearance

The PANI and PANI/SD/TiO$_2$ synthesized were observed to be granulated powders with green and light green colours respectively. It has been reported that the shape, appearance and colour of PANI composites or hybrids are dependent on dopants / substances used [30]. The various composites have been reported to appear as greenish coloured compounds such as PANI/TiO$_2$ which has been reported to be dark green [31]. The colour variations have been explained extensively in the literature as resulting from protonation and deprotonation of the PANI.

3.2. Structural Characterization

The structure of the synthesized PANI/SD/TiO$_2$ was characterized by FTIR and UV-vis spectroscopy and compared to pristine PANI (Fig.1). The characteristic peaks of the pure PANI (Fig. 1a) at 1400 cm^{-1} and 1500 cm^{-1} were attributed to C-C stretching of the benzenoid and C=N stretching of the quinoid rings respectively. These characteristics bands were similarly reported in other studies [32]. The characteristic absorption band around 1193 cm^{-1} [33] related to the C–N stretching in bipolaron

structure was observed [34]. The peak at 1280 cm^{-1} corresponding to C–N stretching of secondary amine in polymer main chain was observed and has been reported by Hatchett et.al. [35]. The existence of absorption band at 805 cm^{-1} was interpreted as originating from out of plane bending vibration of C–H, which is formed in the aromatic ring structure during the protonation of HCl-doped PANI [36]. These results indicate that the synthesised PANI was highly doped and existed in conducting emeraldine salt form. For the PANI/SD/TiO$_2$, the characteristic PANI bands were red shifted. The C-N stretch initially at 1193 cm^{-1} for pure PANI was observed at 1198 cm^{-1} for PANI/SD/TiO$_2$ composite. In addition to these, C-N stretching observed at 1280 cm^{-1} for pure PANI was shifted to 1297 cm^{-1} for PANI/SD/TiO$_2$ composite. The aromatic C-H stretching bands at 805 cm^{-1} in pure PANI shifted to higher wave numbers of 817 cm^{-1} for PANI/SD/TiO$_2$ composite relative to pristine PANI. Also the characteristic peak at 1400 cm^{-1} observed in PANI was slightly red shifted to 1401 cm^{-1}. It was also observed that the introduction of SD and TiO$_2$ into the pure PANI matrix caused significant reductions in the intensity of the aromatic peak. These changes in intensity and wavelength shifts were due to changes in π electron delocalisation in the aromatic rings; the shift towards higher wavenumber indicates an increase in the conjugation length as a result of doping with an electron reach dopant. Both the amine and imine group of PANI are affected by dopant exchange. Thus, changing wavelength of both C-C and C=N stretching [37]. These peak red-shifted can also be due to PANI transition from the emeralidine base (EB) to the emeralidine salt (ES) during the doping process or morphological changes [37]. These changes confirm that they are structural and morphological changes in PANI in PANI/SD/TIO$_2$ composite as results of interactions of the compounds in the composites.
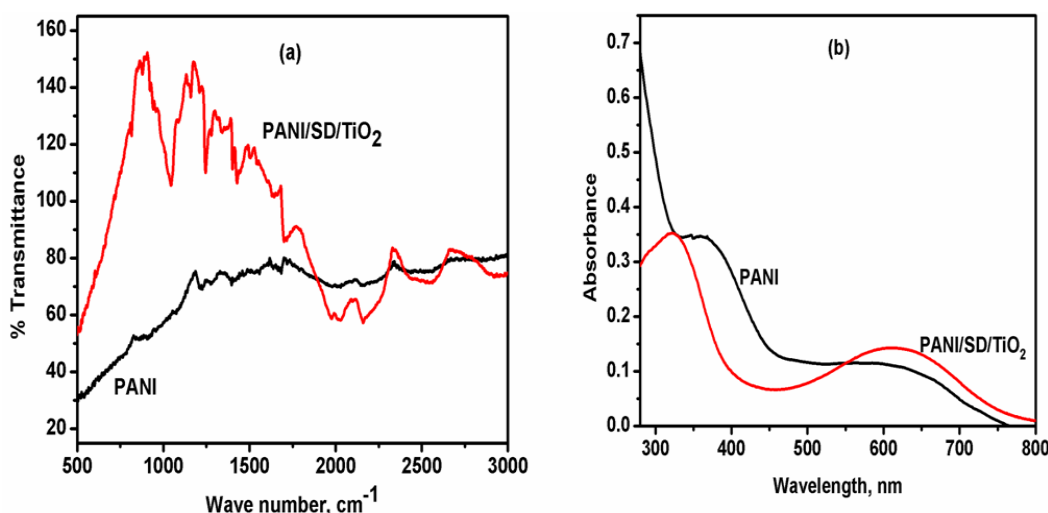

Figure 1: Spectrophotometric spectra for the polyanilines a) FTIR and b) UV- visible

Fig. 1(b) shows the UV-vis spectra of PANI/SD/TiO$_2$ powders. The absorption bands at 294 and 386 nm in PANI (Fig. 1b) were attributed to π-π* transitions in the benzenoid structure [38] which are typical of the analyzed

materials. These bands exhibited red shifts (bathochromic shift) to 389 nm in PANI/SD/TiO$_2$ as observed in Fig. 1b. The shoulder at 526 nm in PANI describes the benzenoid to quinoid ring excitonic transition [39]. This corresponds to

the n-π* transitions of quinine-imine groups [40]. This shoulder experiences a red shift to 537 nm in PANI/SD/TiO$_2$. The presence of a peak and a shoulder in PANI spectra was indicative of the presence of two types of chemically non-equivalent rings in the polymer chain, namely the benzenoid and the quinoid rings [41]. From the spectra of the composites, it was observed that the intensity of π–π* transition peak and excitonic transition peak increased with red shifts compared to that of pristine PANI. However, this increase was quite high in the excitonic transition peak and rather low in the π–π* transition peak. This suggested that SD and TiO$_2$ particles had some interactions with quinoid rings on the polymer and these affected the excitonic transition peak and resulted in a possible complexation. These interactions reduce the band gap of π–π* transition of rings which existed in the polymer structure and thus electron transitions occur with lower energy.

3.3. Morphology

The morphologies of the synthesized PANI/SD/TiO$_2$ were investigated by SEM and TEM observations. The morphology composites and the qualitative dispersion of the TiO$_2$ and SD particles in the composites were examined by SEM. SEM micrograph of PANI and its composites are shown in Fig. 2a. PANI powder appeared to have numerous honeycombed structures with observable pores within the polymer matrix as similarly reported by Chao [42]. The micrograph of the neat PANI powder revealed plain, homogeneous and condense powder surfaces.

PANI/SD/TiO$_2$ composite was noted to be similar, with cauliflower shape and had heaped pores structures as shown in Fig. 2a. The micrographs of PANI/SD/TiO$_2$ clearly indicated that the TiO$_2$ and SD particles were well dispersed (Fig. 2a). This was due to interactions from the charge transfer of nitrogen atom of the quinoid units of the polymer to SD and TiO$_2$ particles [43]. Although the morphology of the composite did not differ much from the pure PANI, when TiO$_2$ was added, the grain size of composite became smaller, which led to the changes in morphological structure; heaped composites from loose cotton to firm gravel in appearance. Salem et.al has attributed this phenomenon to indicate that the TiO$_2$ particles had a nucleation effect on the polymerization, leading to a homogeneous polyaniline shell around it [44]. The porosity observed in pure PANI structure was retained in PANI/SD/TiO$_2$. Fig. 3b shows the TEM micrographs of (a) pure PANI, and (b) PANI/SD/TiO$_2$ particles. From Fig. 3b, it was observed that the shapes of the polymers varied. PANI had networked rod structures and PANI/SD/TiO$_2$ had aggregated rod like structures, respectively. The TEM image of the PANI/SD/TiO$_2$ composites in Fig. 3b showed smeared dark spheres due to the doped PANI, which was similar to the results obtained by Wei et.al.[45]. The surfaces of the PANI/SD/TiO$_2$ hybrid particles were different from those of the pure PANI due to the interpenetration of PANI in SD structure as shown in Fig. 3b. The resultant PANI/SD/TiO$_2$ material therefore showed well dispersed particles of SD and TiO$_2$ around the polyaniline backbone structure.
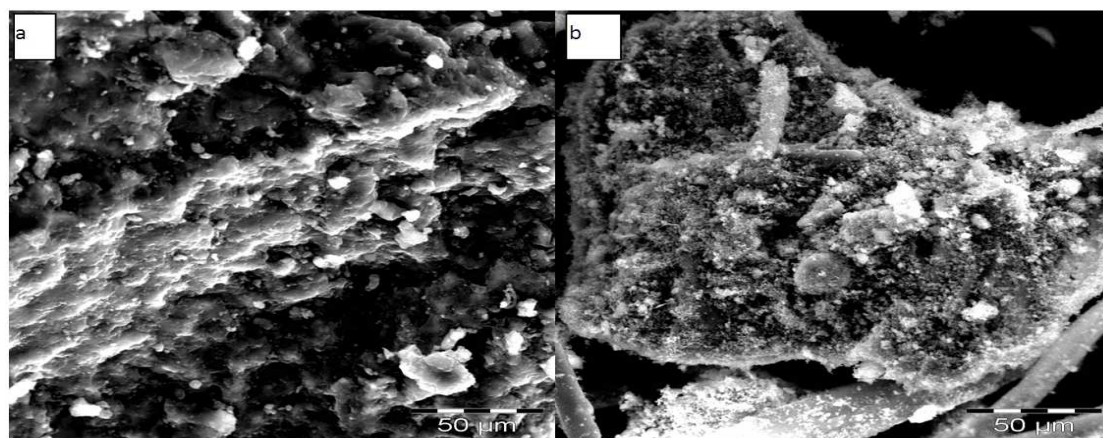

Figure 2: SEM micrograms of the polyanilines a) PANI and b) PANI/SW/TiO$_2$composite

3.4. Physical Characterization

Fig. 4a represents the TGA curves of the polyanilines determined through weight loss (%) data obtained between 30 and 400 °C. It was observed that the PANIs showed two-step mass loss processes which were similar to the reported observations [46]. The first process around 60 to 140 °C was attributed to the expulsion of water and dopant from the PANI matrix. The second step mass loss occurring between 160 and 400 °C varied depending on the composite and most of the weight losses occurred here.

This step was due to the degradation of PANI backbone. The first weight loss at 60 °C provided the weight composition of PANI versus the dopant (SD and TiO$_2$) components, and the second weight loss provided information regarding the influence of the SD and TiO$_2$ on the thermal properties of the polymer composites relative to pure PANI. The degradation of the PANI/SD/TiO$_2$ occurred at 20 °C lower than the degradation temperature of pure PANI suggesting that the composite influenced the structure and thermal stability of PANI [47]. The weight losses in PANI/SD/TiO$_2$ between 30-150 °C were thought

to be due to the presence of unremoved water molecules as moisture in polymers and PANI composites and acid dopants [48]. The onset of the decomposition of PANI was at 150 °C while that for PANI/SD/TiO$_2$ occurred at 260 °C. Since the decomposition of PANI/SD/TiO$_2$ started at a higher temperature, it suggests that this composite is stable as indicated by the TGA results.

XRD technique was used to identify the hybrid nature of the polymer materials in which crystalline orientation of synthesized polymers was studied. Fig. 4b shows the X-ray diffraction patterns of PANI and PANI/SD/TiO$_2$ composites. Pure PANI powders exhibited two broad peaks at 2θ angles of 20 ° and 26 °, which indicated that PANI contained some crystalline domains [49]. These peaks may be assigned to the scattering from PANI chains at interplanar spacing [50].

The PANI characteristic peak at 26 ° was associated to the amorphous structure of PANI [51]. In PANI/SD/TiO$_2$ patterns, it was observed that the diffraction peaks appeared at 2θ values of 25 °, 37 °, 47 °, 53 °, 61 °, 68 ° and 75 ° which were associated with presence of TiO$_2$ phase [31]. These are weak and narrow peaks suggesting that the formation of PANI/SD/TiO$_2$ with the crystalline structures. However, the effects of SD and TiO$_2$ in the PANI/SD/TiO$_2$ composite with TiO$_2$ might have been more predominant than SD causing the material to be crystalline. By comparing the XRD patterns of the composite and pure PANI, it was confirmed that PANI retained its structure even though it was distorted during the polymerization reaction.
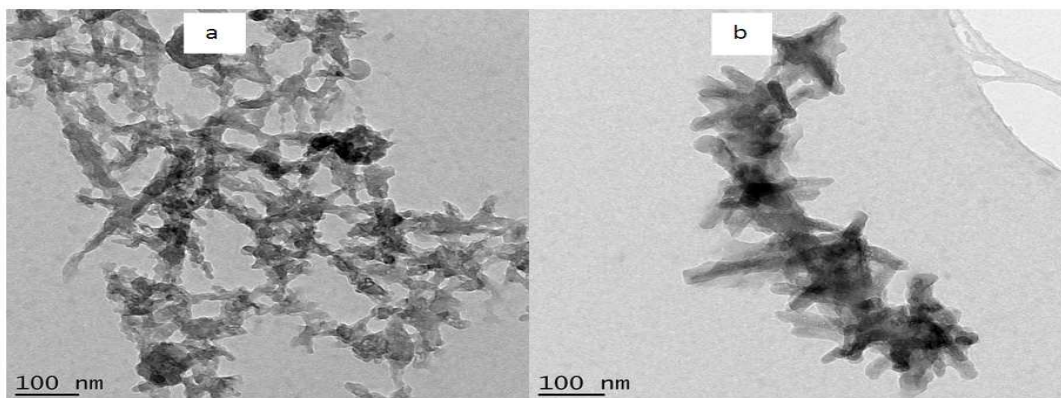

Figure3: *TEM images of the polyanilines a) PANI and b) PANI/SW/TiO$_2$ composite*

3.5. Adsorption Studies

The experiment was done at different time intervals between 0 to 120 min with a fixed adsorbent dose of 0.05 g PANI/SD/TiO$_2$. Below Fig. 5 depicts that the uptake of PCBs by PANI/SD/TiO$_2$ was quite rapid initially, gradually slowed down and then reached equilibrium. From the plot it was evident that a substantial amount was adsorbed within 0 to 15 min of contact time with PANI/SD/TiO$_2$ in all the PCBs analysed relative to subsequent periods thereafter. PCB 28 reached equilibrium much earlier at 45 min while 75 min was taken for the attainment of equilibrium for PCB 52, with PCB 101 attained its equilibrium adsorption after 90 min. Adsorption occurred at a faster rate for PCB 28 compared to PCB 52 and PCB 101 which suggested a preference of lower chlorinated congeners (PCB 28) relative to the high substituted congener (PCB 101).

The extraction studies were further evaluated by comparison of voltammograms of analytes obtained before and after adsorption (inserts in Fig. 5). From these inserts it they were no observable reduction peaks in the voltammograms, which is an indication of absence of detectable PCB's. This confirms the potential of the synthesized adsorbent materials for PCB remediation.

The adsorption capacities were calculated as 8.09 mg g^{-1} (PCB 28), 4.58 mg g^{-1} (PCB 52) and 3.76 mg g^{-1} (PCB 101)

as shown in Table 1. From studies of partition coefficients, the adsorption of PCB 21 and PCB 173 was reported to increase as the lipophilic character of the compounds increase [2]. Since solubility decreases with the number of chlorines attached to the biphenyl molecule. This is similar to the results observed in this study with PCB 28 tending to be more lipophilic relative to PCB 52 and PCB 101 and adsorbs faster as shown in Fig. 5.). A similar relationship where a lower adsorption capacity for the highly chlorinated PCB mixtures, in comparison with the less chlorinated ones, has been reported elsewhere [52]. An observation of preferential coplanar sorption was also reported elsewhere for PCB interaction with humic substrates [53].

3.6. Kinetics of Adsorption

According to the kinetic data obtained from the experiments, pseudo-second-order and Intraparticle diffusion equation were used to explain the adsorption mechanism. The validities of these four kinetic models are checked and depicted in Fig. 6 (a-c) which was based on linearized equations;

1. Pseudo-second-order equation:

$$\frac{t}{q_t} = \frac{1}{k_2 q_e^2} + \frac{t}{q_e} \qquad (2)$$

Where q_e and q_t are the amounts of PCB adsorbed (mole g^{-1}) at equilibrium and at time t (min), k_2 is the rate constant of pseudo-second order sorption and t is the adsorption time (min). For the pseudo-second-order model used in PCB 28 and PCB 52, a plot t/q_t versus t should give a straight line and q_e and k_2 can be determined from the slope and intercept of the plot respectively.

2.   Intraparticle diffusion equation:

$$q_e = K_1 t^{0.5} + C \tag{3}$$

Where C is the intercept, related to the thickness of the boundary layer and k_i is the intraparticle diffusion rate constant. For all the models evaluated, the determination coefficient r^2 was applied to determine which of the kinetic models linear best fitted the data. Regarding the Intraparticle diffusion model used in PCB 101, the values of constants C were obtained from the intercept of the

straight line plot of qt versus $t^{0.5}$. For this model, it is essential that when the intraparticle diffusion is the sole rate-limiting step [54], a plot of q_t vs. $t^{0.5}$ is a straight line passing through the origin.

Other kinetic model equations applied include;

3.   Pseudo-first-order equation:

$$\log(q_e - q_t) = \log q_e - \frac{K_1 t}{2.303} \tag{4}$$

Where q_e and q_t are the amounts of PCB adsorbed (mole g^{-1}) at equilibrium and at time t (min), k_1 is the rate constant of pseudo-first order sorption and t is the adsorption time (min).

4.   Elovich equation:

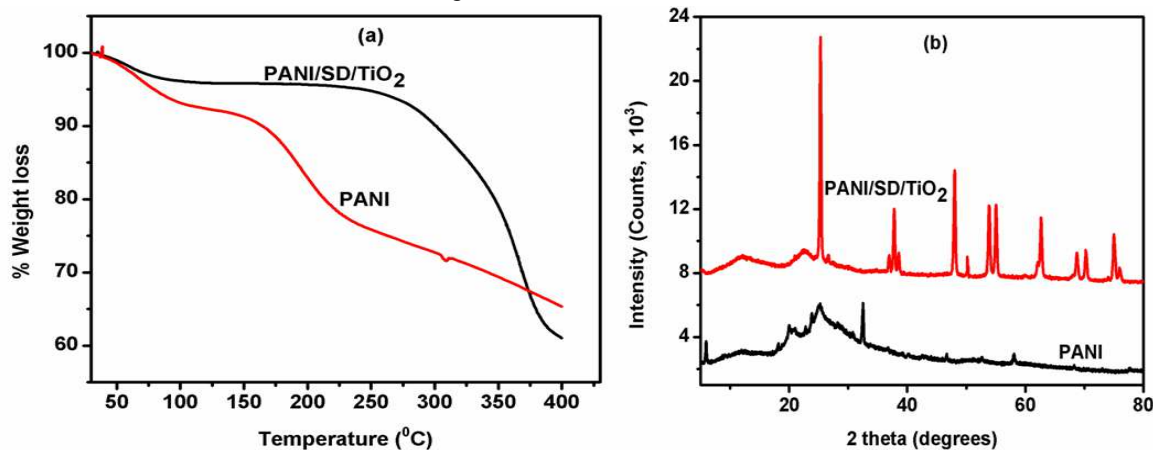$$q_t = b + aInt \tag{5}$$

Figure 4: *Thermal and physical properties of the Polyanilines A) TGA curves and b) XRD patterns*

Where q_t is the amount of PCB adsorbed (mole g^{-1}) at time t (min), b and a are the desorption constant (g mol^{-1}) and initial sorption rate (mol g^{-1} min^{-1}) respectively and t is the adsorption time (min).

Based on linear regression (R^2) values, the adsorption kinetics of PCBs onto PANI/SD/TiO$_2$ can be described well

by pseudo-second order and intraparticle diffusion models (Fig. 6). Comparison of other two kinetic models (Eqn. 4 and 5) did not yield better results compared to Equation 2 and 3 (Table I). The corresponding kinetic parameters and the correlation coefficients are summarized in Table 1.
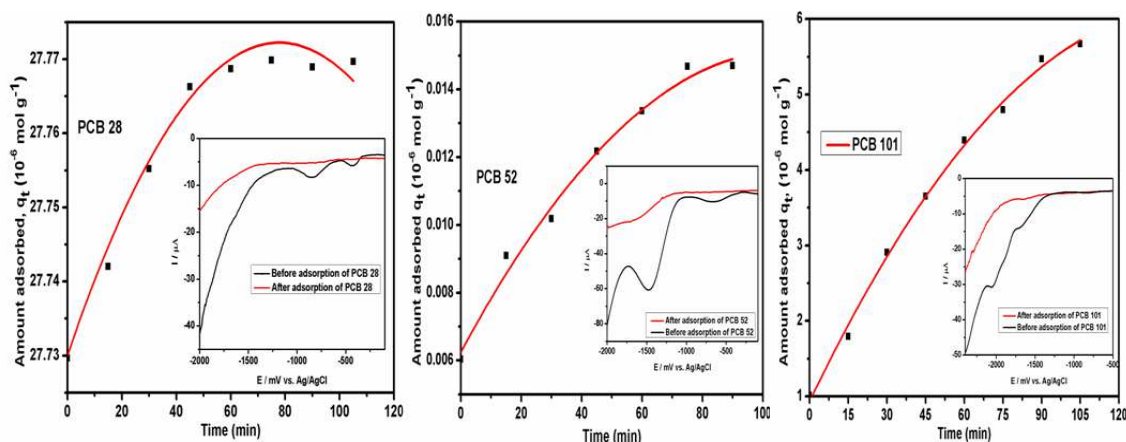

Figure 5: *Effect of contact time on adsorption of PCBs onto PANI/SD/TiO$_2$; (0.05g Solid, at 25 °C, 1.75 h) and insets are voltammogram comparison of before and after adsorption for each PCB analyte*

Table 1: Summary of the kinetic and isotherm parameters for adsorption of PCBs: parameters are explained in the text

Kinetics model	Parameter	PCB 28	PCB 52	PCB 101
	K_1/min	0.023	0.007	0.015
Pseudo first -order	$Q_{e\,cal}$ (mol g^{-1})	1.89×10^{-5}	6.212×10^{-6}	4.540×10^{-5}
	R^2	0.916	0.928	0.846
	K_2 (gmol^{-1} min^{-1})	2.41×10^2	91.95	286.73
Pseudo second -order	$Q_{e\,cal}$ (mol g^{-1})	2.77×10^{-5}	1.57×10^{-5}	1.88×10^{-5}
	R^2,	0.991	0.962	0.848
	K_1 (mol g^{-1}min$^{-0.5}$)	4×10^{-9}	1×10^{-9}	6.95×10^{-7}
Intraparticle Diffusion	C (mol g^{-1})	3×10^{-9}	6×10^{-9}	1.77×10^{-6}
	R^2	0.892	0.910	0.992
	a	1×10^{-8}	7×10^{-9}	2×10^{-6}
Elovich	b	3×10^{-5}	1×10^{-9}	2×10^{-5}
	R^2	0.845	0.855	0.907
Isotherm	Langmuir (R^2)	0.999	0.986	0.954
	Freundlich (R^2)	0.955	0.994	0.910
Adsorption Capacity (mg g^{-1})		8.09	4.58	3.76

For our kinetic data, r^2, and the quantity adsorbed at equilibrium q_e were calculated and estimated as shown in Table 1. The linear fits obtained by applying the pseudo second order model with the determination coefficient values ranged from 0.991 (PCB 28) to 0.962 (PCB 52) indicating that the kinetics behaviour was better approximated to the pseudo-second-order kinetics and for PCB 101 intraparticle diffusion model, it was found to fit with coefficient value of 0.992. For this model the rate constant (k_2) decrease with increasing chlorination, which could be attributed to the increased number of chloride ions available for adsorption.
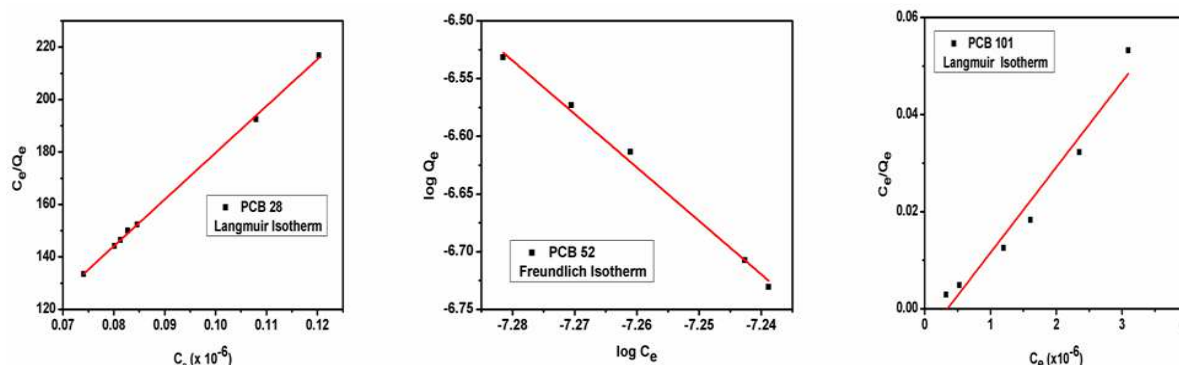
Results of the kinetic models used showed good correlation coefficients for pseudo-second-order kinetic model and supported the fact that adsorption of PCB congeners (PCB 28 and PCB 52) onto functionalized polyaniline coated sawdust follows a pseudo-second-order model (Fig. 6). This kinetic model is associated with chemisorption mechanism as argued in past literature where Pirbazari and Weber [52] mentioned that adsorption of PCBs on carbon may be predominantly chemisorption. In the case of PCB 101, the kinetic model that explained the nature of adsorption process here was found to be intraparticle diffusion model which suggested a possible diffusion limited step during adsorption.

3.7. Adsorption Isotherm

Results of adsorption equilibrium for PCB 28, PCB 52, and PCB 101 are shown in Fig. 5. The experimental results were analyzed by linear Langmuir and Freundlich isotherm models, two widely used models. Generally, Freundlich isotherm is empirical, whereas the Langmuir isotherm is the simplest theoretical model for monolayer adsorption onto a surface with finite number of identical sites Langmuir isotherm. The model assumes uniform energies of adsorption onto the surface and no transmigration of adsorbate in the plane of the surface. The linear form of the Langmuir isotherm is given by Eq. (6):

$$\frac{C_e}{q_e} = \frac{C_e}{q_{max}} + \frac{1}{kq_{max}} \qquad (6)$$

Where q_e is the amount adsorbed per mass of adsorbent (mg g^{-1}), q_{max} is the monolayer capacity (mg g^{-1}), C_e is the equilibrium concentration (mg L^{-1}) and k is a constant that is related to the energy of adsorption. Thus, a plot of C_e/q_e versus C_e is expected to give a straight line of slope $1/q_{max}$ and intercepts $1/kq_{max}$. From the results of this plot, regression coefficient values of PCB 28 (0.999) and PCB 101 (0.954) were obtained which indicates that the data best fitted the Langmuir isotherm. These results indicate that the adsorption of the selected PCBs by PANI/SD/TiO$_2$ did not follow one adsorption isotherm but varied.

Figure 6: The best Kinetic models observed for the three PCB congeners

Freundlich isotherm. Freundlich expression is an empirical equation applicable to non-ideal sorption on heterogeneous surface as well as multilayer sorption [55]. For Freundlich isotherm, a linear expression form for the equation is given by;

$$\log q_e = \frac{1}{k_f} + \frac{1}{n} \log C_e \qquad (7)$$

Therefore, a plot of $\ln q_e$ versus $\ln C_e$ should be a straight line of slope $1/n$ and intercept l/k_f where q_e is the amount adsorbed per mass of adsorbent, k_f is the Freundlich constant, C_e is the equilibrium concentration and $1/n$ is interpreted as a heterogeneity factor [56]. The Freundlich plot gave a straight line with $R^2 > 0{:}994$ which show that the adsorption of PCB 52 follows the Freundlich isotherm. The equations above were demonstrated differently for each isotherm study.

The Langmuir equation did not reproduce equilibrium data satisfactorily for PCB 52 which could be attributed to the energetic heterogeneity of the PANI/SD/TiO$_2$ as similarly reported [57]. However, a better reproduction was obtained for PCB 28 and PCB 101, indicating that the ranges of adsorption energy for these compounds were narrower than that for PCB 52. The Freundlich isotherm led to reasonably good results for the PCB 52 (Fig. 6) which was similar to results of PCB 52 adsorption onto fly ash [57]. Research has shown that the adsorption capacity of non-coplanar hydrophobic organic compounds (HOCs) was lower than that of co-planar compounds of similar hydrophobicity on various forms of black carbon [58, 59]. The adsorption attenuation was attributed to steric hindrances, presumably brought about by the twisting of biphenyl rings with respect to one another as more chlorine is added to the structure. A similar analogy can be used to analyse the above data.

4. Conclusion

This study demonstrated the potential of PANI/SD/TiO$_2$ to extract PCBs from contaminated media. PCBs adsorption followed pseudo-second order for PCB 28 and PCB 52 with PCB 101 adsorption obeyed intraparticle diffusion model. PANI/SD/TiO$_2$ adsorbent was used successfully for removal of selected PCB congeners. The adsorption capacity for the lower chlorinated PCB 28 was higher than the adsorption capacity for PCB 52 and PCB 101. Even though not all the 209 PCB congeners were tested, the results so far with 3 selected congeners strongly support the promising ability of the PANI/SD/TiO$_2$ to effectively extract various PCB congeners and give some insights on adsorption behaviour of PCBs on PANI/SD/TiO$_2$. The potential of the synthesized adsorbent to remediate PCBs was assessed with outstanding results. Out of the results discussed above it is clear that PANI/SD/TiO$_2$ can be used to remove PCBs from wastewaters.

References

[1]   J.L. Sotelo, G. Ovejero, J.A. Delgado, I. Martinez. Water Res. 36 (2002) 599-608

[2]   H. Nollet, M. Roels, P. Lutgen, P. Van der Meeren, W. Verstraete. Chemosphere. 53 (2003) 655-665

[3]   C.G. Wu, C. DeGroot, H.O. Marcy, J.L. Schindler, C.R. Kannewurf, Y.J. Liu, W. Hirpo, M.G. Kanatzidis. Chem. Mater. 8 (1996) 1992-2004

[4]   X. Qu, M. Tian, B. Liao, A. Chen. Electrochim. Acta. 55 (2010) 5367-5374

[5]   S.H. Lin, R.S. Juang.. J. Environ. Manage. 90 (2009) 1336-1349

[6]   M. Sahin, H. Gorcay, E. Kir, Y. Sahin. Funct. Polym., 69 (2009) 673-680

[7]   R. Kunin. Pure & Appl. Chem. 46 (1976) 205-211

[8]   A.M. Li, Q.X. Zhang, G.C. Zhang, J.L. Chen, Z.H. Fei, F.Q. Liu. Chemosphere. 47 (9) (2002) 981-989

[9]   B.J. Pan, B.C. Pan, W.M. Zhang, Q.X. Zhang, S.R. Zhang, S.R. Zheng, J. Hazard. Mater. 157 (2008) 293-299

[10] J. Huang, C. Yan, K. Huang.J. Colloid Interface Sci., 332 (1) (2009) 60-64

[11] B.L. He, W.Q. Huang. Shanghai Scientific and Technical Education, Shanghai, (1995) 439-452

[12] S. Meada , S.P.Armes. Synth. Met. 73 (1995) 151

[13] A-N. Chowdhury ,M.A Yousuf , M.M. Rahman. Indian J. Chem., 41A (2002) 1562

[14] A.B Smith, C.J Knowles. J. Biotechnol. Appl. Biochem. 12(1990) 661

[15] B.Miksa , S. Slomkowski. Colloid Polym. Sci.273 (1995) 47.

[16] A.N. Chowdhury, S. R. Jesmeen and M. M. Hossain. Polym. Adv. Technol. 15(2004) 633–638

[17] M. M. Ayad and A. A. El-Nas. J. Phys. Chem 114 (2010), 14377–1438

[18] P.A. Kumar, S. Chakraborty and M. Ray. Chem. Eng. J. 141 (2008) 130–140

[19] D.S. Minehan, K.A Marx , S.K Tripathy . Macromolecules 27(1994) 777

[20] B. Saoudi, N. Jammul, M.M. Chehimi, G.P. McCarthy,

S.P.Armes. J. Colloid Interface Sci. 192(1997) 269

[21] B. Saoudi, N. Jammul, M-L. Abel, M.M. Chehimi, G. Dodin. Synth. Met. 87(1997) 97

[22] R. Ansari, F. Raofie. CODEN ECJHAO E-J., of Chem., 3 (10) (2006a) 49-59

[23] R. Ansari, F. Raofie, CODEN ECJHAO E-J. of Chem., 3 (10) (2006b) 35-43

[24] R. Ansari, N. K. Fahim, A. F. Delavar, The Open Process Chem. J., 2 (2009) 1-5

[25] R. Ansari, Z. Mosayebzadeh, Iran. Polym. J. 19 (7) (2010) 541-551

[26] H.J. Walther, J. Kaeding, P. Fecimer, Acta. Hydrochim. Hydrobiol. 12 (2) (1984) 173-181

[27] M. Dore, P. Simon, A. Deguin, J. Victor, Water Res. 20(2) (1986) 221-232

[28] M. Barletta, A. Gisario, G. Rubino, V. Tagliaferri, Tech. 201 (2006) 3212-3228

[29] T.T. Waryo, E.A. Songa, M.C. Matoetoe, R.F. Ngece, P.M. Ndangili, A. AlAhmed, N.M. Jahed, P.G.L. Baker, E.I. Iwuoha. Chapter 2, Nanostructured Materials for Electrochemical Biosensors, New York: Nova Science Publishers (2009)

[30] Q.M. Pham, D.H. Pham, J.S. Kim, E.J. Kim, S. Kim. Synth. Met. 159 (19-20) (2009) 2141-2146

[31] S. Quillard, G. Louarn, S. Lefrant and A.G. MacDiarmid.Phys. Rev. B50 (17) (1994) 12496-12508

[32] A.G. MacDiarmid, J.C. Chiang, M. Halpern, W.S. Huang, S.L. Mu, N.L.D. Somasiri, W.Q. Wu and S.I. Yaniger, Mol. Cryst. Liq. Cryst. 121 (1985) 173-180

[33] P.S. Khiew, N.M. Huang, S. Radiman and M.S. Ahmad. Mater. Lett. 58 (2004) 516-521

[34] D.W. Hatchett, M. Josowicz and J. Janata. J. Phys. Chem. B103 (1999) 10992-10998

[35] M.G. Han, S.K. Cho, S.G. Oh and S.S. Im. Synth. Met. 126(1) (2002) 53-60

[36] M. Trchová and J. Stejskal. Pure Appl. Chem., Vol. 83 (10) (2011) 1803–1817

[37] M.K. Ram, O. Yavuz, V. Lahsangah and M. Aldissi. Sens. Actuators. B106 (2005) 750-757.

[38] Y. Xia, M. Wiesinger and A.G. MacDiarmid. Chem. Mater. 7(3) (1995) 443-445

[39] J. Stejskal, D. Hlavata, P. Holler, M. Trchova, J. Prokes and

I. Sapurina. Polym. Int. 53 (2004) 294-300

[40] P. Rannou, A. Gawlicka, D. Berner, A. Pron, M. Nechtschein and D. Djurado, Macromolecules. 31(9) (1998) 3007-3015

[41] D. Chao, J. Chen, X. Lu, L. Liang Chen, W. Zhang, and Y. Wei. Synth. Met. 150 (2005) 47-51.

[42] H. Zengin and G. Kalayci. Mater. Chem. Phys. 120 (2010) 46-53

[43] M.A. Salem, A.F. Al-Ghonemiy and A.B. Zaki. Appl. Catal. B: Environ. 91 (2009) 59-66

[44] C. Wei, Y. Zhu, X. Yang and C. Li. Mater. Sci. Eng. B: Solid-State Mater. Adv. Technol. 137(1-3) (2007) 213-216.

[45] M.C. Gupta and S.S. Umare, Studies on poly (omethoxyaniline). Macromolecules. 25 (1992) 138-142

[46] S. Wang, Z. Tan, Y. Li, L. Sun and T. Zhang. Thermochim. Acta. 441 (2006) 191-194

[47] M. Ghorbani and H. Eisazadeh. Synth. Met. 162 (2002) 527-530

[48] W. Pan, S.L. Yang, G. Li and J.M. Jiang. Eur. Polym. J. 41 (2005) 2127-2133

[49] W. Feng, E. Sun, A. Fujii, H. Wu, K. Niihara and K. Yoshinno. Bull. Chem. Soc. Jpn. 73 (2000) 2627-2633

[50] Z. Zhang, Z. Wei and M. Wan,. Macromolecules. 35 (15) (2002) 5937-5942

[51] M. Pirbazari, W.J. Weber. Chemistry Water Reuse, vol. 2. Cooper N.J. (ed.) USA: Ann Arbor Science, (1981) 309-339

[52] M.E. Uhle, Y.P. Chin, G.R. Aiken. Environ. Sci. Technol. 33 (1999) 2715-2718.

[53] G. Bia, C.P. De Pauli, L. Borgnino. J. Environ. Manage. 100 (2012) 1-9

[54] M.A. Abdullah, L. Chiang, M. Nadeem. Chem. Eng. J. 146 (2009) 370-376

[55] S.L.C. Ferreira, H.M.C. Andrade, H.C. dos Santos. J. Colloid Interface Sci. 270 (2004) 276-280

[56] T.H. Yoon, K. Benzerara, S. Ahn, R.G. Luthy, T. Tyliszczak, G.E. Brown. Environ. Sci. Technol. 40 (19) (2006) 54

[57] M.T.O. Jonker, A.A. Koelmans. Environ. Sci. Technol. 36 (2002) 3725-3734.

[58] G. Cornelissen, O. Gustafsson. Environ. Sci. Technol. 38 (1) (2004) 148-155. 923-5929

[59] H. Nollet, M. Roels, P. Lutgen, P. Van der Meeren, W. Verstraete. Chemosphere. 53 (2003) 655–665